Sparsity in Astrophysics

Astrostatistics meets Astroinformatics

Jason McEwen
www.jasonmcewen.org
@jasonmcewen

Mullard Space Science Laboratory (MSSL)
University College London (UCL)

With thanks to my collaborators Laura Wolz, Filipe Abdalla, Rafael Carrillo & Yves Wiaux

8th International Conference of the ERCIM on Computational and Methodological Statistics
London, December 2015

Next-generation of radio interferometry rapidly approaching

- Square Kilometre Array (SKA) construction scheduled to begin 2018.
- Many other pathfinder telescopes under construction, *e.g.* LOFAR, ASKAP, MeerKAT, MWA.
- Broad range of science goals.

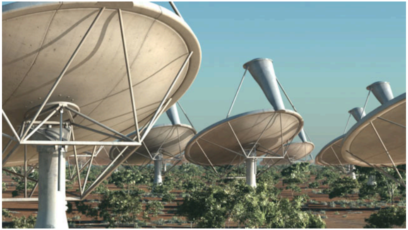

Figure: Artist impression of SKA dishes. [Credit: SKA Organisation]

Next-generation of radio interferometry rapidly approaching

- Square Kilometre Array (SKA) construction scheduled to begin 2018.
- Many other pathfinder telescopes under construction, *e.g.* LOFAR, ASKAP, MeerKAT, MWA.
- Broad range of science goals.

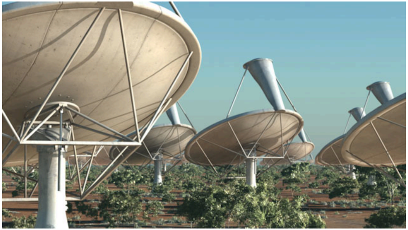

Figure: Artist impression of SKA dishes. [Credit: SKA Organisation]

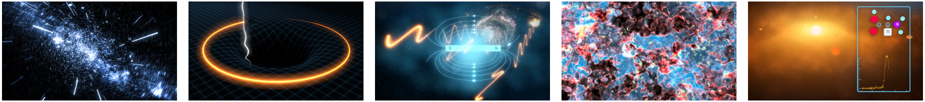

(a) Dark-energy (b) GR (c) Cosmic magnetism (d) Epoch of reionization (e) Exoplanets

Figure: SKA science goals. [Credit: SKA Organisation]

SKA sites

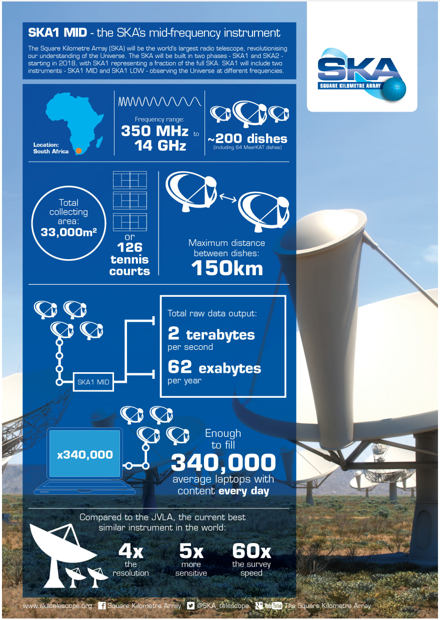
SKA1 MID - the SKA's mid-frequency instrument
The Square Kilometre Array (SKA) will be the world's largest radio telescope, revolutionising our understanding of the Universe. The SKA will be built in two phases - SKA1 and SKA2 - starting in 2018, with SKA1 representing a fraction of the full SKA. SKA1 will include two instruments - SKA1 MID and SKA1 LOW - observing the Universe at different frequencies.
SKA SQUARE KILOMETRE ARRAY
Location: South Africa
Frequency range:
350 MHz to 14 GHz
~200 dishes
(including 64 MeerKAT dishes)
Total collecting area: 33,000m²
or 126 tennis courts
Maximum distance between dishes: 150km
SKA1 MID
Total raw data output:
2 terabytes per second
62 exabytes per year
x340,000
Enough to fill 340,000 average laptops with content every day
Compared to the JVLA, the current best similar instrument in the world:
4x the resolution
5x more sensitive
60x the survey speed
www.skatelescope.org Square Kilometre Array @SKA_telescope The Square Kilometre Array

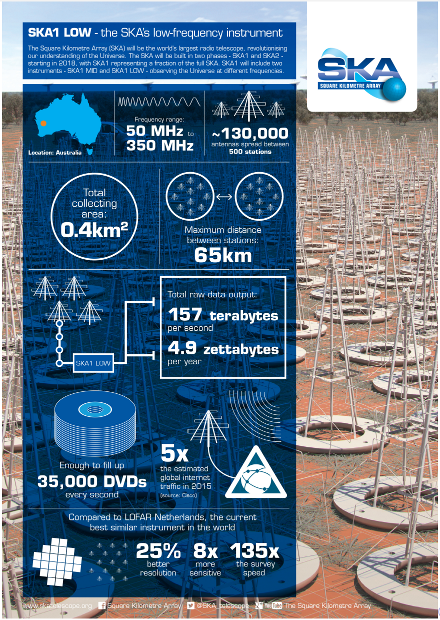
SKA1 LOW - the SKA's low-frequency instrument
The Square Kilometre Array (SKA) will be the world's largest radio telescope, revolutionising our understanding of the Universe. The SKA will be built in two phases - SKA1 and SKA2 - starting in 2018, with SKA1 representing a fraction of the full SKA. SKA1 will include two instruments - SKA1 MID and SKA1 LOW - observing the Universe at different frequencies.
SKA SQUARE KILOMETRE ARRAY
Location: Australia
Frequency range:
50 MHz to 350 MHz
~130,000 antennas spread between 500 stations
Total collecting area: 0.4km²
Maximum distance between stations: 65km
SKA1 LOW
Total raw data output:
157 terabytes per second
4.9 zettabytes per year
Enough to fill up 35,000 DVDs every second
5x the estimated global internet traffic in 2015
(source: Cisco)
Compared to LOFAR Netherlands, the current best similar instrument in the world
25% better resolution
8x more sensitive
135x the survey speed
www.skatelescope.org Square Kilometre Array @SKA_telescope The Square Kilometre Array

The SKA poses a considerable big-data challenge

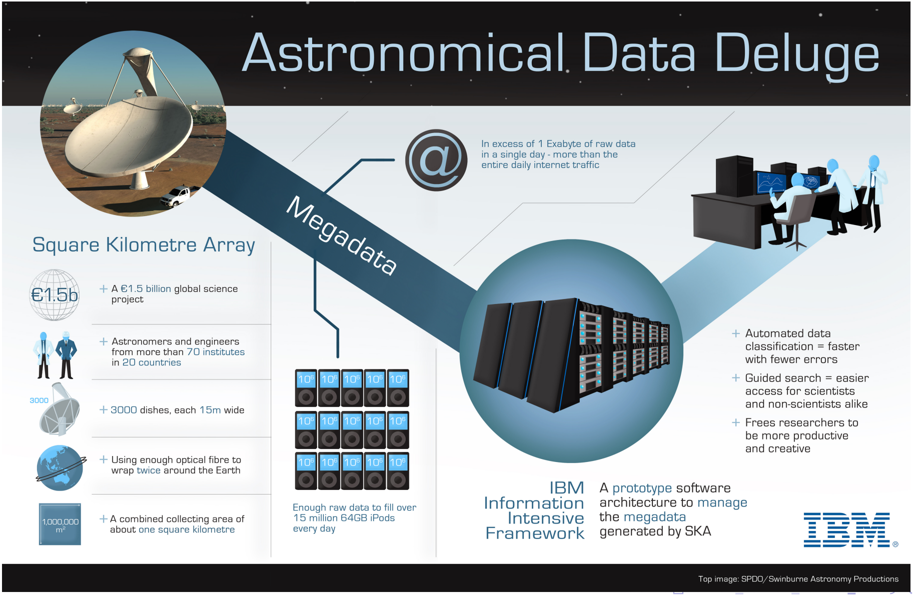

The SKA poses a considerable big-data challenge

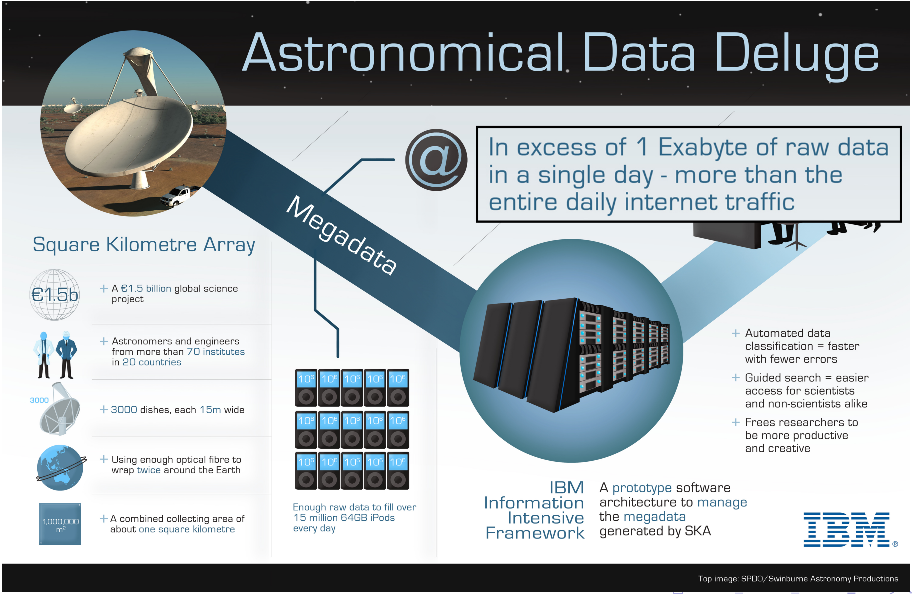

Outline

1. Compressive sensing and sparse regularisation
   - Introductory review
   - Analysis vs synthesis
   - Bayesian interpretations

2. Interferometric imaging with compressive sensing
   - Imaging with the SARA algorithm
   - Continuous visibilities
   - Spread spectrum effect

Outline

1. Compressive sensing and sparse regularisation
   - Introductory review
   - Analysis vs synthesis
   - Bayesian interpretations

2. Interferometric imaging with compressive sensing
   - Imaging with the SARA algorithm
   - Continuous visibilities
   - Spread spectrum effect

Compressive sensing

- Developed by Candes *et al.* 2006 and Donoho 2006 (and others).
- Although many underlying ideas around for a long time.
- Exploits the sparsity of natural signals.
- Active area of research with many new developments.
- Acquisition versus imaging.

(a) Emmanuel Candes

(b) David Donoho

Compressive sensing

- Developed by Candes *et al.* 2006 and Donoho 2006 (and others).
- Although many underlying ideas around for a long time.
- Exploits the sparsity of natural signals.
- Active area of research with many new developments.
- Acquisition versus imaging.

(a) Emmanuel Candes

(b) David Donoho

An introduction to compressive sensing

Operator description

- Linear operator (linear algebra) representation of signal decomposition:

$$x(t) = \sum_i \alpha_i \Psi_i(t) \quad \rightarrow \quad \boldsymbol{x} = \sum_i \Psi_i \alpha_i = \begin{pmatrix} | \\ \Psi_0 \\ | \end{pmatrix} \alpha_0 + \begin{pmatrix} | \\ \Psi_1 \\ | \end{pmatrix} \alpha_1 + \cdots \quad \rightarrow \quad \boxed{\boldsymbol{x} = \Psi \boldsymbol{\alpha}}$$

- Linear operator (linear algebra) representation of measurement:

$$y_i = \langle x, \Phi_j \rangle \quad \rightarrow \quad \boldsymbol{y} = \begin{pmatrix} - \Phi_0 - \\ - \Phi_1 - \\ \vdots \end{pmatrix} \boldsymbol{x} \quad \rightarrow \quad \boxed{\boldsymbol{y} = \Phi \boldsymbol{x}}$$

- Putting it together: $\boxed{\boldsymbol{y} = \Phi \boldsymbol{x} = \Phi \Psi \boldsymbol{\alpha}}$

An introduction to compressive sensing

Operator description

- Linear operator (linear algebra) representation of signal decomposition:

$$x(t) = \sum_i \alpha_i \Psi_i(t) \quad \rightarrow \quad \boldsymbol{x} = \sum_i \Psi_i \alpha_i = \begin{pmatrix} | \\ \Psi_0 \\ | \end{pmatrix} \alpha_0 + \begin{pmatrix} | \\ \Psi_1 \\ | \end{pmatrix} \alpha_1 + \cdots \quad \rightarrow \quad \boxed{\boldsymbol{x} = \Psi \boldsymbol{\alpha}}$$

- Linear operator (linear algebra) representation of measurement:

$$y_i = \langle x, \Phi_j \rangle \quad \rightarrow \quad \boldsymbol{y} = \begin{pmatrix} - & \Phi_0 & - \\ - & \Phi_1 & - \\ & \vdots & \end{pmatrix} \boldsymbol{x} \quad \rightarrow \quad \boxed{\boldsymbol{y} = \Phi \boldsymbol{x}}$$

- Putting it together: $\boxed{\boldsymbol{y} = \Phi \boldsymbol{x} = \Phi \Psi \boldsymbol{\alpha}}$

An introduction to compressive sensing

Operator description

- Linear operator (linear algebra) representation of signal decomposition:

$$x(t) = \sum_i \alpha_i \Psi_i(t) \quad \rightarrow \quad \boldsymbol{x} = \sum_i \Psi_i \alpha_i = \begin{pmatrix} | \\ \Psi_0 \\ | \end{pmatrix} \alpha_0 + \begin{pmatrix} | \\ \Psi_1 \\ | \end{pmatrix} \alpha_1 + \cdots \quad \rightarrow \quad \boxed{\boldsymbol{x} = \Psi \boldsymbol{\alpha}}$$

- Linear operator (linear algebra) representation of measurement:

$$y_i = \langle x, \Phi_j \rangle \quad \rightarrow \quad \boldsymbol{y} = \begin{pmatrix} - \ \Phi_0 \ - \\ - \ \Phi_1 \ - \\ \vdots \end{pmatrix} \boldsymbol{x} \quad \rightarrow \quad \boxed{\boldsymbol{y} = \Phi \boldsymbol{x}}$$

- Putting it together: $\boxed{\boldsymbol{y} = \Phi \boldsymbol{x} = \Phi \Psi \boldsymbol{\alpha}}$

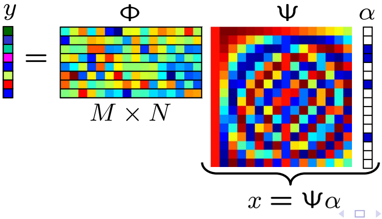

An introduction to compressive sensing

Promoting sparsity via ℓ_1 minimisation

- Ill-posed inverse problem:

$$\boldsymbol{y} = \Phi \boldsymbol{x} + \boldsymbol{n} = \Phi \Psi \boldsymbol{\alpha} + \boldsymbol{n} .$$

- Solve by imposing a regularising prior that the signal to be recovered is sparse in Ψ, *i.e.* solve the following ℓ_0 optimisation problem:

$$\boldsymbol{\alpha}^\star = \arg\min_{\boldsymbol{\alpha}} \|\alpha\|_0 \text{ such that } \|\boldsymbol{y} - \Phi \Psi \boldsymbol{\alpha}\|_2 \leq \epsilon ,$$

where the signal is synthesising by $\boldsymbol{x}^\star = \Psi \boldsymbol{\alpha}^\star$.

- Recall norms given by:

$$\|\alpha\|_0 = \text{no. non-zero elements} \qquad \|\alpha\|_1 = \sum_i |\alpha_i| \qquad \|\alpha\|_2 = \Big(\sum_i |\alpha_i|^2\Big)^{1/2}$$

- Solving this problem is difficult (combinatorial).
- Instead, solve the ℓ_1 optimisation problem (convex):

$$\boldsymbol{\alpha}^\star = \arg\min_{\boldsymbol{\alpha}} \|\alpha\|_1 \text{ such that } \|\boldsymbol{y} - \Phi \Psi \boldsymbol{\alpha}\|_2 \leq \epsilon .$$

An introduction to compressive sensing

Promoting sparsity via ℓ_1 minimisation

- Ill-posed inverse problem:

$$\boldsymbol{y} = \Phi \boldsymbol{x} + \boldsymbol{n} = \Phi \Psi \boldsymbol{\alpha} + \boldsymbol{n} .$$

- Solve by imposing a regularising prior that the signal to be recovered is sparse in Ψ, *i.e.* solve the following ℓ_0 optimisation problem:

$$\boldsymbol{\alpha}^\star = \arg\min_{\boldsymbol{\alpha}} \|\alpha\|_0 \text{ such that } \|\boldsymbol{y} - \Phi\Psi\boldsymbol{\alpha}\|_2 \leq \epsilon ,$$

  where the signal is synthesising by $\boldsymbol{x}^\star = \Psi \boldsymbol{\alpha}^\star$.

- Recall norms given by:

$$\|\alpha\|_0 = \text{no. non-zero elements} \qquad \|\alpha\|_1 = \sum_i |\alpha_i| \qquad \|\alpha\|_2 = \Big(\sum_i |\alpha_i|^2\Big)^{1/2}$$

- Solving this problem is difficult (combinatorial).

- Instead, solve the ℓ_1 optimisation problem (convex):

$$\boldsymbol{\alpha}^\star = \arg\min_{\boldsymbol{\alpha}} \|\alpha\|_1 \text{ such that } \|\boldsymbol{y} - \Phi\Psi\boldsymbol{\alpha}\|_2 \leq \epsilon .$$

An introduction to compressive sensing

Promoting sparsity via ℓ_1 minimisation

- Ill-posed inverse problem:

$$\boxed{\boldsymbol{y} = \Phi \boldsymbol{x} + \boldsymbol{n} = \Phi \Psi \boldsymbol{\alpha} + \boldsymbol{n}} \, .$$

- Solve by imposing a regularising prior that the signal to be recovered is sparse in Ψ, *i.e.* solve the following ℓ_0 optimisation problem:

$$\boxed{\boldsymbol{\alpha}^\star = \underset{\boldsymbol{\alpha}}{\arg\min} \|\alpha\|_0 \;\text{ such that }\; \|\boldsymbol{y} - \Phi\Psi\boldsymbol{\alpha}\|_2 \leq \epsilon} \, ,$$

where the signal is synthesising by $\boldsymbol{x}^\star = \Psi \boldsymbol{\alpha}^\star$.

- Recall norms given by:

$$\|\alpha\|_0 = \text{no. non-zero elements} \qquad \|\alpha\|_1 = \sum_i |\alpha_i| \qquad \|\alpha\|_2 = \Big(\sum_i |\alpha_i|^2\Big)^{1/2}$$

- Solving this problem is difficult (combinatorial).

- Instead, solve the ℓ_1 optimisation problem (convex):

$$\boxed{\boldsymbol{\alpha}^\star = \underset{\boldsymbol{\alpha}}{\arg\min} \|\alpha\|_1 \;\text{ such that }\; \|\boldsymbol{y} - \Phi\Psi\boldsymbol{\alpha}\|_2 \leq \epsilon} \, .$$

An introduction to compressive sensing

Promoting sparsity via ℓ_1 minimisation

- Ill-posed inverse problem:

$$\boxed{\boldsymbol{y} = \Phi \boldsymbol{x} + \boldsymbol{n} = \Phi \Psi \boldsymbol{\alpha} + \boldsymbol{n}} \, .$$

- Solve by imposing a regularising prior that the signal to be recovered is sparse in Ψ, *i.e.* solve the following ℓ_0 optimisation problem:

$$\boxed{\boldsymbol{\alpha}^\star = \arg\min_{\boldsymbol{\alpha}} \|\alpha\|_0 \ \text{ such that } \ \|\boldsymbol{y} - \Phi\Psi\boldsymbol{\alpha}\|_2 \leq \epsilon} \, ,$$

where the signal is synthesising by $\boldsymbol{x}^\star = \Psi \boldsymbol{\alpha}^\star$.

- Recall norms given by:

$$\|\alpha\|_0 = \text{no. non-zero elements} \qquad \|\alpha\|_1 = \sum_i |\alpha_i| \qquad \|\alpha\|_2 = \Big(\sum_i |\alpha_i|^2\Big)^{1/2}$$

- Solving this problem is difficult (combinatorial).
- Instead, solve the ℓ_1 optimisation problem (convex):

$$\boxed{\boldsymbol{\alpha}^\star = \arg\min_{\boldsymbol{\alpha}} \|\alpha\|_1 \ \text{ such that } \ \|\boldsymbol{y} - \Phi\Psi\boldsymbol{\alpha}\|_2 \leq \epsilon} \, .$$

An introduction to compressive sensing

Union of subspaces

- Space of sparse vectors given by the union of subspaces aligned with the coordinate axes.

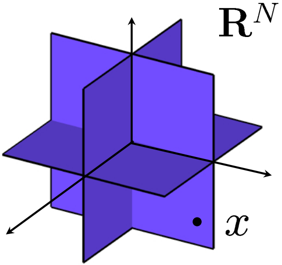

Figure: Space of the sparse vectors [Credit: Baraniuk]

An introduction to compressive sensing

Restricted isometry property (RIP)

- Solutions of ℓ_0 and ℓ_1 problems often the same.
- Restricted isometry property (RIP):

$$(1-\delta_{2K})\|\boldsymbol{x}_1-\boldsymbol{x}_2\|_2^2 \leq \|\Theta\boldsymbol{x}_1-\Theta\boldsymbol{x}_2\|_2^2 \leq (1+\delta_{2K})\|\boldsymbol{x}_1-\boldsymbol{x}_2\|_2^2 \,,$$

  for K-sparse $\boldsymbol{x}_1$ and $\boldsymbol{x}_2$, where $\Theta=\Phi\Psi$.
- Measurement must preserve geometry of sets of sparse vectors.

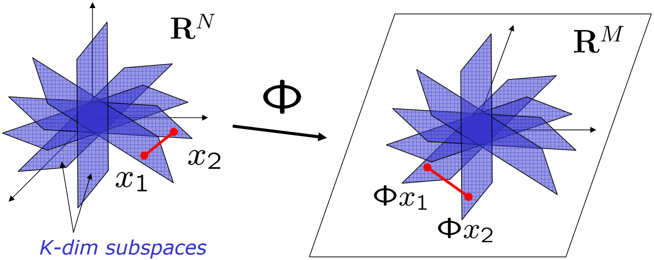

Figure: Measurement must preserve geometry of sets of sparse vectors. [Credit: Baraniuk]

An introduction to compressive sensing
Intuition

- Solutions of ℓ_0 and ℓ_1 problems often the same.
- Geometry of ℓ_0, ℓ_2 and ℓ_1 problems.

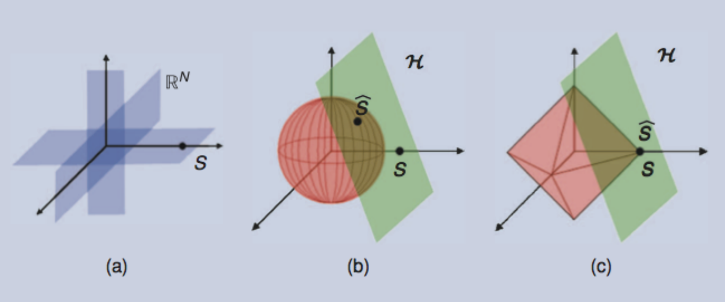

Figure: Geometry of (a) ℓ_0 (b) ℓ_2 and (c) ℓ_1 problems. [Credit: Baraniuk (2007)]

An introduction to compressive sensing

Sparsity and coherence

- Number of measurements required to achieve exact reconstruction is given by

$$\boxed{M \geq c\mu^2 K \log N} \, ,$$

  where K is the sparsity and N the dimensionality.

- The coherence between the measurement and sparsity basis is given by

$$\boxed{\mu = \sqrt{N} \max_{i,j} |\langle \Psi_i, \Phi_j \rangle|} \, .$$

An introduction to compressive sensing

Sparsity and coherence

- Number of measurements required to achieve exact reconstruction is given by

$$M \geq c\mu^2 K \log N ,$$

  where K is the sparsity and N the dimensionality.

- The coherence between the measurement and sparsity basis is given by

$$\mu = \sqrt{N} \max_{i,j} |\langle \Psi_i, \Phi_j \rangle| .$$

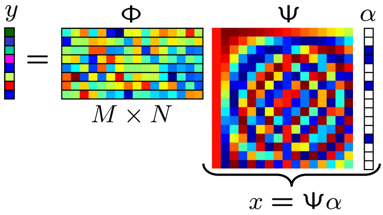

Analysis vs synthesis

- Typically sparsity assumption is justified by analysing example signals in terms of atoms of the dictionary.
- But this is different to synthesising signals from atoms.
- Suggests an analysis-based framework (Elad *et al.* 2007, Nam *et al.* 2012):

$$x^\star = \arg\min_{x} \|\Omega x\|_1 \text{ such that } \|y - \Phi x\|_2 \leq \epsilon \,.$$

analysis

- Contrast with synthesis-based approach:

$$x^\star = \Psi \cdot \arg\min_{\alpha} \|\alpha\|_1 \text{ such that } \|y - \Phi\Psi\alpha\|_2 \leq \epsilon \,.$$

synthesis

- For orthogonal bases $\Omega = \Psi^\dagger$ and the two approaches are identical.

Analysis vs synthesis

- Typically sparsity assumption is justified by analysing example signals in terms of atoms of the dictionary.
- But this is different to synthesising signals from atoms.
- Suggests an analysis-based framework (Elad *et al.* 2007, Nam *et al.* 2012):

$$\boldsymbol{x}^\star = \underset{\boldsymbol{x}}{\arg\min} \, \|\Omega \boldsymbol{x}\|_1 \;\; \text{such that} \;\; \|\boldsymbol{y} - \Phi \boldsymbol{x}\|_2 \leq \epsilon \, .$$

analysis

- Contrast with synthesis-based approach:

$$\boldsymbol{x}^\star = \Psi \cdot \underset{\boldsymbol{\alpha}}{\arg\min} \, \|\boldsymbol{\alpha}\|_1 \;\; \text{such that} \;\; \|\boldsymbol{y} - \Phi \Psi \boldsymbol{\alpha}\|_2 \leq \epsilon \, .$$

synthesis

- For orthogonal bases $\Omega = \Psi^\dagger$ and the two approaches are identical.

Analysis vs synthesis

- Typically sparsity assumption is justified by analysing example signals in terms of atoms of the dictionary.
- But this is different to synthesising signals from atoms.
- Suggests an analysis-based framework (Elad *et al.* 2007, Nam *et al.* 2012):

$$\boldsymbol{x}^\star = \underset{\boldsymbol{x}}{\arg\min} \|\Omega \boldsymbol{x}\|_1 \ \text{ such that } \ \|\boldsymbol{y} - \Phi \boldsymbol{x}\|_2 \leq \epsilon \,.$$

analysis

- Contrast with synthesis-based approach:

$$\boldsymbol{x}^\star = \Psi \ \cdot \ \underset{\boldsymbol{\alpha}}{\arg\min} \|\boldsymbol{\alpha}\|_1 \ \text{ such that } \ \|\boldsymbol{y} - \Phi \Psi \boldsymbol{\alpha}\|_2 \leq \epsilon \,.$$

synthesis

- For orthogonal bases $\Omega = \Psi^\dagger$ and the two approaches are identical.

Analysis vs synthesis

- Typically sparsity assumption is justified by analysing example signals in terms of atoms of the dictionary.
- But this is different to synthesising signals from atoms.
- Suggests an analysis-based framework (Elad *et al.* 2007, Nam *et al.* 2012):

$$\boldsymbol{x}^\star = \underset{\boldsymbol{x}}{\arg\min} \, \|\Omega \boldsymbol{x}\|_1 \ \text{such that} \ \|\boldsymbol{y} - \Phi \boldsymbol{x}\|_2 \leq \epsilon \, .$$

analysis

- Contrast with synthesis-based approach:

$$\boldsymbol{x}^\star = \Psi \cdot \underset{\boldsymbol{\alpha}}{\arg\min} \, \|\boldsymbol{\alpha}\|_1 \ \text{such that} \ \|\boldsymbol{y} - \Phi \Psi \boldsymbol{\alpha}\|_2 \leq \epsilon \, .$$

synthesis

- For orthogonal bases $\Omega = \Psi^\dagger$ and the two approaches are identical.

Analysis vs synthesis
Comparison

- Synthesis-based approach is more general, while analysis-based approach more restrictive.

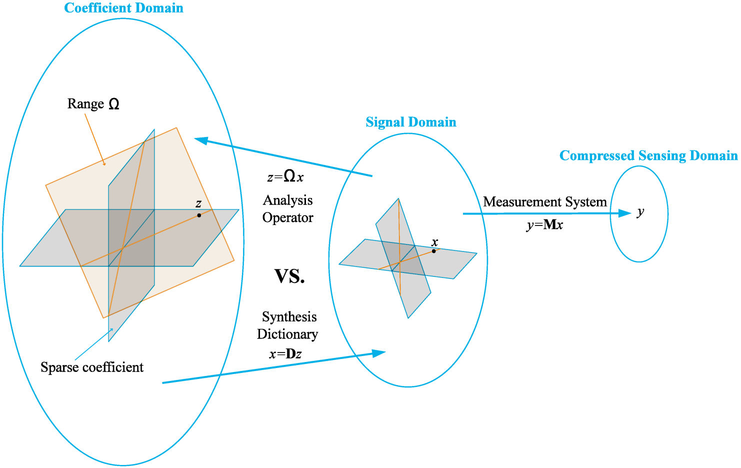

Figure: Analysis- and synthesis-based approaches [Credit: Nam *et al.* (2012)].

Bayesian interpretations

One Bayesian interpretation of the synthesis-based approach

- Consider the inverse problem:

$$\boldsymbol{y} = \Phi\Psi\boldsymbol{\alpha} + \boldsymbol{n} \, .$$

- Assume Gaussian noise, yielding the likelihood:

$$\mathrm{P}(\boldsymbol{y} \,|\, \boldsymbol{\alpha}) \propto \exp\left(\|\boldsymbol{y} - \Phi\Psi\boldsymbol{\alpha}\|_2^2 / (2\sigma^2) \right) \, .$$

- Consider the Laplacian prior:

$$\mathrm{P}(\boldsymbol{\alpha}) \propto \exp\left(-\beta \|\boldsymbol{\alpha}\|_1 \right) \, .$$

- The maximum *a-posteriori* (MAP) estimate (with $\lambda = 2\beta\sigma^2$) is

$$\boldsymbol{x}^\star_{\text{MAP-Synthesis}} = \Psi \cdot \underset{\boldsymbol{\alpha}}{\arg\max}\, \mathrm{P}(\boldsymbol{\alpha} \,|\, \boldsymbol{y}) = \Psi \cdot \underset{\boldsymbol{\alpha}}{\arg\min}\, \|\boldsymbol{y} - \Phi\Psi\boldsymbol{\alpha}\|_2^2 + \lambda \|\boldsymbol{\alpha}\|_1 \, .$$

synthesis

- One possible Bayesian interpretation!
- Signal may be ℓ_0-sparse, then solving ℓ_1 problem finds the correct ℓ_0-sparse solution!

Bayesian interpretations

One Bayesian interpretation of the synthesis-based approach

- Consider the inverse problem:

$$\boldsymbol{y} = \Phi\Psi\boldsymbol{\alpha} + \boldsymbol{n} \, .$$

- Assume Gaussian noise, yielding the likelihood:

$$\mathrm{P}(\boldsymbol{y} \,|\, \boldsymbol{\alpha}) \propto \exp\Big(\|\boldsymbol{y} - \Phi\Psi\boldsymbol{\alpha}\|_2^2 / (2\sigma^2) \Big) \, .$$

- Consider the Laplacian prior:

$$\mathrm{P}(\boldsymbol{\alpha}) \propto \exp\Big(-\beta \|\boldsymbol{\alpha}\|_1 \Big) \, .$$

- The maximum *a-posteriori* (MAP) estimate (with $\lambda = 2\beta\sigma^2$) is

$$\boldsymbol{x}^\star_{\text{MAP-Synthesis}} = \Psi \cdot \underset{\boldsymbol{\alpha}}{\arg\max}\, \mathrm{P}(\boldsymbol{\alpha} \,|\, \boldsymbol{y}) = \Psi \cdot \underset{\boldsymbol{\alpha}}{\arg\min}\, \|\boldsymbol{y} - \Phi\Psi\boldsymbol{\alpha}\|_2^2 + \lambda \|\boldsymbol{\alpha}\|_1 \, .$$

synthesis

- One possible Bayesian interpretation!
- Signal may be ℓ_0-sparse, then solving ℓ_1 problem finds the correct ℓ_0-sparse solution!

Bayesian interpretations

One Bayesian interpretation of the synthesis-based approach

- Consider the inverse problem:

$$\boldsymbol{y} = \Phi\Psi\boldsymbol{\alpha} + \boldsymbol{n} \, .$$

- Assume Gaussian noise, yielding the likelihood:

$$\mathrm{P}(\boldsymbol{y} \,|\, \boldsymbol{\alpha}) \propto \exp\Big(\|\boldsymbol{y} - \Phi\Psi\boldsymbol{\alpha}\|_2^2 / (2\sigma^2)\Big) \, .$$

- Consider the Laplacian prior:

$$\mathrm{P}(\boldsymbol{\alpha}) \propto \exp\Big(-\beta\|\boldsymbol{\alpha}\|_1\Big) \, .$$

- The maximum *a-posteriori* (MAP) estimate (with $\lambda = 2\beta\sigma^2$) is

$$\boldsymbol{x}^{\star}_{\text{MAP-Synthesis}} = \Psi \cdot \underset{\boldsymbol{\alpha}}{\arg\max}\, \mathrm{P}(\boldsymbol{\alpha} \,|\, \boldsymbol{y}) = \Psi \cdot \underset{\boldsymbol{\alpha}}{\arg\min}\, \|\boldsymbol{y} - \Phi\Psi\boldsymbol{\alpha}\|_2^2 + \lambda\|\boldsymbol{\alpha}\|_1 \, .$$

synthesis

- One possible Bayesian interpretation!
- Signal may be ℓ_0-sparse, then solving ℓ_1 problem finds the correct ℓ_0-sparse solution!

Bayesian interpretations

Other Bayesian interpretations of the synthesis-based approach

- Other Bayesian interpretations are also possible (Gribonval 2011).
- Minimum mean square error (MMSE) estimators
  - ⊂ synthesis-based estimators with appropriate penalty function, *i.e.* penalised least-squares (LS)
  - ⊂ MAP estimators

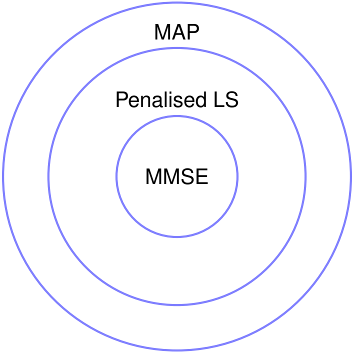

Bayesian interpretations

One Bayesian interpretation of the analysis-based approach

- For the analysis-based approach, the MAP estimate is then

$$\boldsymbol{x}^{\star}_{\text{MAP-Analysis}} = \arg\max_{\boldsymbol{x}} \mathrm{P}(\boldsymbol{x} \,|\, \boldsymbol{y}) = \arg\min_{\boldsymbol{x}} \|\boldsymbol{y} - \Phi\boldsymbol{x}\|_2^2 + \lambda\|\Omega\boldsymbol{x}\|_1 \ .$$

analysis

- Identical to the synthesis-based approach if $\Omega = \Psi^{\dagger}$.

- But for redundant dictionaries, the analysis-based MAP estimate is

$$\boldsymbol{x}^{\star}_{\text{MAP-Analysis}} = \Omega^{\dagger} \cdot \arg\min_{\boldsymbol{\gamma} \in \text{column space } \Omega} \|\boldsymbol{y} - \Phi\Omega^{\dagger}\boldsymbol{\gamma}\|_2^2 + \lambda\|\boldsymbol{\gamma}\|_1 \ .$$

analysis

- Analysis-based approach more restrictive than synthesis-based.

- Similar ideas promoted by Maisinger & Hobson (2004) in a Bayesian framework for wavelet MEM (maximum entropy method).

Bayesian interpretations

One Bayesian interpretation of the analysis-based approach

- For the analysis-based approach, the MAP estimate is then

$$\boxed{x^\star_{\text{MAP-Analysis}} = \arg\max_{x} \mathrm{P}(x \mid y) = \arg\min_{x} \|y - \Phi x\|_2^2 + \lambda \|\Omega x\|_1 \ .}$$

analysis

- Identical to the synthesis-based approach if $\Omega = \Psi^\dagger$.
- But for redundant dictionaries, the analysis-based MAP estimate is

$$\boxed{x^\star_{\text{MAP-Analysis}} = \Omega^\dagger \cdot \arg\min_{\gamma \in \text{column space } \Omega} \|y - \Phi \Omega^\dagger \gamma\|_2^2 + \lambda \|\gamma\|_1 \ .}$$

analysis

- Analysis-based approach more restrictive than synthesis-based.
- Similar ideas promoted by Maisinger & Hobson (2004) in a Bayesian framework for wavelet MEM (maximum entropy method).

Bayesian interpretations

One Bayesian interpretation of the analysis-based approach

- For the analysis-based approach, the MAP estimate is then

$$\boxed{x^{\star}_{\text{MAP-Analysis}} = \arg\max_{x} \mathrm{P}(x \mid y) = \arg\min_{x} \|y - \Phi x\|_2^2 + \lambda \|\Omega x\|_1 \; .}$$

analysis

- Identical to the synthesis-based approach if $\Omega = \Psi^{\dagger}$.
- But for redundant dictionaries, the analysis-based MAP estimate is

$$\boxed{x^{\star}_{\text{MAP-Analysis}} = \Omega^{\dagger} \cdot \arg\min_{\gamma \in \text{column space } \Omega} \|y - \Phi \Omega^{\dagger} \gamma\|_2^2 + \lambda \|\gamma\|_1 \; .}$$

analysis

- Analysis-based approach more restrictive than synthesis-based.
- Similar ideas promoted by Maisinger & Hobson (2004) in a Bayesian framework for wavelet MEM (maximum entropy method).

Bayesian interpretations

One Bayesian interpretation of the analysis-based approach

- For the analysis-based approach, the MAP estimate is then

$$\boldsymbol{x}^\star_{\text{MAP-Analysis}} = \arg\max_{\boldsymbol{x}} \mathrm{P}(\boldsymbol{x} \,|\, \boldsymbol{y}) = \arg\min_{\boldsymbol{x}} \|\boldsymbol{y} - \Phi\boldsymbol{x}\|_2^2 + \lambda\|\Omega\boldsymbol{x}\|_1 \ .$$

analysis

- Identical to the synthesis-based approach if $\Omega = \Psi^\dagger$.

- But for redundant dictionaries, the analysis-based MAP estimate is

$$\boldsymbol{x}^\star_{\text{MAP-Analysis}} = \Omega^\dagger \cdot \arg\min_{\boldsymbol{\gamma} \in \text{column space } \Omega} \|\boldsymbol{y} - \Phi\Omega^\dagger\boldsymbol{\gamma}\|_2^2 + \lambda\|\boldsymbol{\gamma}\|_1 \ .$$

analysis

- Analysis-based approach more restrictive than synthesis-based.

- Similar ideas promoted by Maisinger & Hobson (2004) in a Bayesian framework for wavelet MEM (maximum entropy method).

Outline

1. Compressive sensing and sparse regularisation
   - Introductory review
   - Analysis vs synthesis
   - Bayesian interpretations

2. Interferometric imaging with compressive sensing
   - Imaging with the SARA algorithm
   - Continuous visibilities
   - Spread spectrum effect

Radio interferometric telescopes acquire “Fourier” measurements

“Fourier”
Measurements

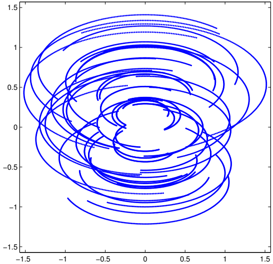

Radio interferometric inverse problem

- Consider the ill-posed inverse problem of radio interferometric imaging:

$$\boxed{\boldsymbol{y} = \Phi \boldsymbol{x} + \boldsymbol{n}} \,,$$

  where $\boldsymbol{y}$ are the measured visibilities, Φ is the linear measurement operator, $\boldsymbol{x}$ is the underlying image and $\boldsymbol{n}$ is instrumental noise.

- Measurement operator $\boxed{\Phi = \mathbf{M}\,\mathbf{F}\,\mathbf{C}\,\mathbf{A}}$ may incorporate:
  - primary beam $\mathbf{A}$ of the telescope;
  - w-modulation modulation $\mathbf{C}$;
  - Fourier transform $\mathbf{F}$;
  - masking $\mathbf{M}$ which encodes the incomplete measurements taken by the interferometer.

Radio interferometric inverse problem

- Consider the ill-posed inverse problem of radio interferometric imaging:

$$\boldsymbol{y} = \Phi \boldsymbol{x} + \boldsymbol{n} ,$$

where $\boldsymbol{y}$ are the measured visibilities, Φ is the linear measurement operator, $\boldsymbol{x}$ is the underlying image and $\boldsymbol{n}$ is instrumental noise.

- Measurement operator $\Phi = \mathbf{M}\,\mathbf{F}\,\mathbf{C}\,\mathbf{A}$ may incorporate:
  - primary beam $\mathbf{A}$ of the telescope;
  - w-modulation modulation $\mathbf{C}$;
  - Fourier transform $\mathbf{F}$;
  - masking $\mathbf{M}$ which encodes the incomplete measurements taken by the interferometer.

Radio interferometric inverse problem

- Consider the ill-posed inverse problem of radio interferometric imaging:

$$\boldsymbol{y} = \Phi \boldsymbol{x} + \boldsymbol{n},$$

where $\boldsymbol{y}$ are the measured visibilities, Φ is the linear measurement operator, $\boldsymbol{x}$ is the underlying image and $\boldsymbol{n}$ is instrumental noise.

- Measurement operator $\Phi = \mathbf{M}\,\mathbf{F}\,\mathbf{C}\,\mathbf{A}$ may incorporate:
  - primary beam $\mathbf{A}$ of the telescope;
  - w-modulation modulation $\mathbf{C}$;
  - Fourier transform $\mathbf{F}$;
  - masking $\mathbf{M}$ which encodes the incomplete measurements taken by the interferometer.

Interferometric imaging: recover an image from noisy and incomplete Fourier measurements.

Interferometric imaging with compressed sensing

- Solve the interferometric imaging problem

$$\boldsymbol{y} = \Phi \boldsymbol{x} + \boldsymbol{n} \quad \text{with} \quad \Phi = \mathbf{M}\,\mathbf{F}\,\mathbf{C}\,\mathbf{A} \, ,$$

by applying a prior on sparsity of the signal in a sparsifying dictionary Ψ.

- Basis Pursuit (BP) denoising problem

$$\boldsymbol{\alpha}^\star = \underset{\boldsymbol{\alpha}}{\arg\min} \|\boldsymbol{\alpha}\|_1 \ \text{such that} \ \|\boldsymbol{y} - \Phi\Psi\boldsymbol{\alpha}\|_2 \leq \epsilon \, , \tag{BPDN}$$

where the image is synthesised by $\boldsymbol{x}^\star = \Psi\boldsymbol{\alpha}^\star$.

Interferometric imaging with compressed sensing

- Solve the interferometric imaging problem

$$\boldsymbol{y} = \Phi \boldsymbol{x} + \boldsymbol{n} \quad \text{with} \quad \Phi = \mathbf{M} \, \mathbf{F} \, \mathbf{C} \, \mathbf{A} ,$$

by applying a prior on sparsity of the signal in a sparsifying dictionary Ψ.

- Basis Pursuit (BP) denoising problem

$$\boldsymbol{\alpha}^\star = \arg\min_{\boldsymbol{\alpha}} \|\alpha\|_1 \ \text{such that} \ \|\boldsymbol{y} - \Phi\Psi\boldsymbol{\alpha}\|_2 \leq \epsilon ,$$

BPDN

where the image is synthesised by $\boldsymbol{x}^\star = \Psi\boldsymbol{\alpha}^\star$.

SARA for radio interferometric imaging

Algorithm

- Sparsity averaging reweighted analysis (SARA) for RI imaging (Carrillo, McEwen & Wiaux 2012)
- Consider a dictionary composed of a concatenation of orthonormal bases, i.e.

$$\Psi = \frac{1}{\sqrt{q}}[\Psi_1, \Psi_2, \ldots, \Psi_q],$$

  thus $\Psi \in \mathbb{R}^{N \times D}$ with $D = qN$.
- We consider the following bases: Dirac (*i.e.* pixel basis); Haar wavelets (promotes gradient sparsity); Daubechies wavelet bases two to eight.
  $\Rightarrow$ concatenation of 9 bases
- Promote average sparsity by solving the reweighted ℓ_1 analysis problem:

$$\min_{\bar{x} \in \mathbb{R}^N} \|W \Psi^T \bar{x}\|_1 \quad \text{subject to} \quad \|y - \Phi \bar{x}\|_2 \leq \epsilon \quad \text{and} \quad \bar{x} \geq 0 \,,$$

  SARA

  where $W \in \mathbb{R}^{D \times D}$ is a diagonal matrix with positive weights.
- Solve a sequence of reweighted ℓ_1 problems using the solution of the previous problem as the inverse weights $\rightarrow$ approximate the ℓ_0 problem.

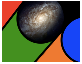

SARA for radio interferometric imaging
Algorithm

- Sparsity averaging reweighted analysis (SARA) for RI imaging (Carrillo, McEwen & Wiaux 2012)

- Consider a dictionary composed of a concatenation of orthonormal bases, i.e.

$$\Psi = \frac{1}{\sqrt{q}} [\Psi_1, \Psi_2, \ldots, \Psi_q],$$

thus $\Psi \in \mathbb{R}^{N \times D}$ with $D = qN$.

- We consider the following bases: Dirac (*i.e.* pixel basis); Haar wavelets (promotes gradient sparsity); Daubechies wavelet bases two to eight.
$\Rightarrow$ concatenation of 9 bases

- Promote average sparsity by solving the reweighted ℓ_1 analysis problem:

$$\min_{\bar{x} \in \mathbb{R}^N} \|W \Psi^T \bar{x}\|_1 \quad \text{subject to} \quad \|y - \Phi \bar{x}\|_2 \leq \epsilon \quad \text{and} \quad \bar{x} \geq 0 \,,$$

SARA

where $W \in \mathbb{R}^{D \times D}$ is a diagonal matrix with positive weights.

- Solve a sequence of reweighted ℓ_1 problems using the solution of the previous problem as the inverse weights $\rightarrow$ approximate the ℓ_0 problem.

SARA for radio interferometric imaging

Algorithm

- Sparsity averaging reweighted analysis (SARA) for RI imaging (Carrillo, McEwen & Wiaux 2012)

- Consider a dictionary composed of a concatenation of orthonormal bases, i.e.

$$\Psi = \frac{1}{\sqrt{q}}[\Psi_1, \Psi_2, \dots, \Psi_q],$$

  thus $\Psi \in \mathbb{R}^{N \times D}$ with $D = qN$.

- We consider the following bases: Dirac (*i.e.* pixel basis); Haar wavelets (promotes gradient sparsity); Daubechies wavelet bases two to eight.
  $\Rightarrow$ concatenation of 9 bases

- Promote average sparsity by solving the reweighted ℓ_1 analysis problem:

$$\min_{\bar{\boldsymbol{x}} \in \mathbb{R}^N} \|W \Psi^T \bar{\boldsymbol{x}}\|_1 \quad \text{subject to} \quad \|\boldsymbol{y} - \Phi \bar{\boldsymbol{x}}\|_2 \leq \epsilon \quad \text{and} \quad \bar{\boldsymbol{x}} \geq 0 \,,$$

  SARA

  where $W \in \mathbb{R}^{D \times D}$ is a diagonal matrix with positive weights.

- Solve a sequence of reweighted ℓ_1 problems using the solution of the previous problem as the inverse weights $\rightarrow$ approximate the ℓ_0 problem.

SARA for radio interferometric imaging

Algorithm

- Sparsity averaging reweighted analysis (SARA) for RI imaging (Carrillo, McEwen & Wiaux 2012)
- Consider a dictionary composed of a concatenation of orthonormal bases, i.e.

$$\Psi = \frac{1}{\sqrt{q}}[\Psi_1, \Psi_2, \ldots, \Psi_q],$$

  thus $\Psi \in \mathbb{R}^{N \times D}$ with $D = qN$.

- We consider the following bases: Dirac (*i.e.* pixel basis); Haar wavelets (promotes gradient sparsity); Daubechies wavelet bases two to eight.
  $\Rightarrow$ concatenation of 9 bases
- Promote average sparsity by solving the reweighted ℓ_1 analysis problem:

$$\min_{\bar{\boldsymbol{x}} \in \mathbb{R}^N} \|W \Psi^T \bar{\boldsymbol{x}}\|_1 \quad \text{subject to} \quad \|\boldsymbol{y} - \Phi \bar{\boldsymbol{x}}\|_2 \leq \epsilon \quad \text{and} \quad \bar{\boldsymbol{x}} \geq 0\,,$$

SARA

  where $W \in \mathbb{R}^{D \times D}$ is a diagonal matrix with positive weights.

- Solve a sequence of reweighted ℓ_1 problems using the solution of the previous problem as the inverse weights $\rightarrow$ approximate the ℓ_0 problem.

SARA for radio interferometric imaging

Results on simulations

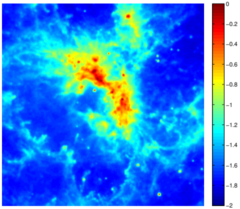

(a) Original

SARA for radio interferometric imaging

Results on simulations

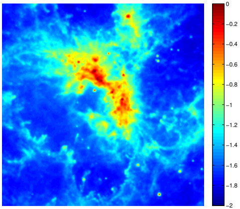

(a) Original

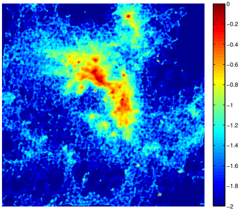

(b) “CLEAN” (SNR=16.67 dB)

SARA for radio interferometric imaging

Results on simulations

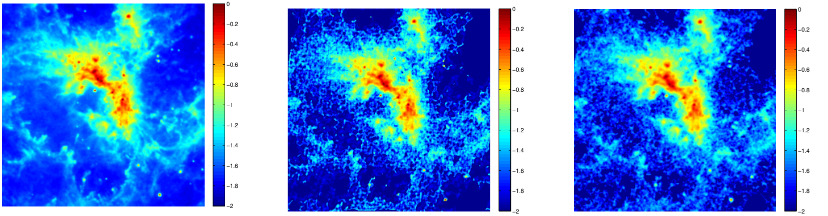

(a) Original (b) “CLEAN” (SNR=16.67 dB) (c) “MS-CLEAN” (SNR=17.87 dB)

SARA for radio interferometric imaging

Results on simulations

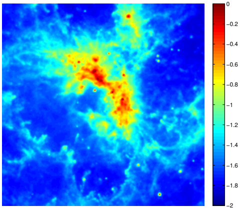

(a) Original

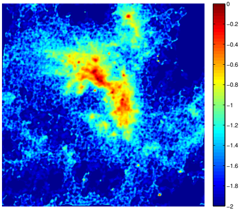

(b) “CLEAN” (SNR=16.67 dB)

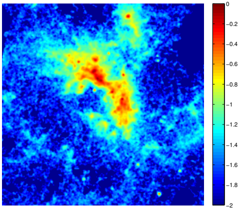

(c) “MS-CLEAN” (SNR=17.87 dB)

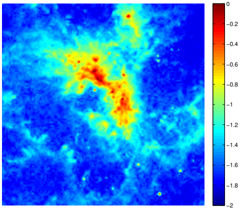

(d) BPDb8 (SNR=24.53 dB)

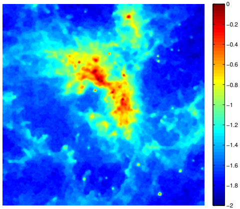

(e) TV (SNR=26.47 dB)

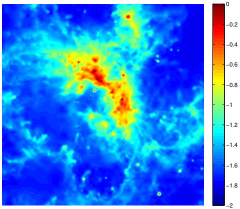

(f) SARA (SNR=29.08 dB)

SARA for radio interferometric imaging

Results on simulations

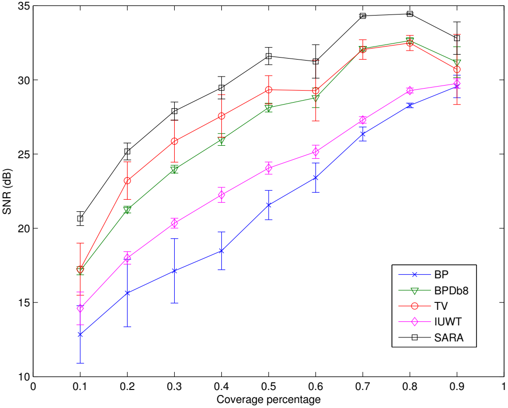

Figure: Reconstruction fidelity vs visibility coverage.

Supporting continuous visibilities

Algorithm

- Ideally we would like to model the continuous Fourier transform operator

$$\boxed{\Phi = \mathbf{F}^{\mathrm{c}}} \, .$$

- But this is impractically slow!
- Incorporated gridding into our CS interferometric imaging framework (Carrillo *et al.* 2014).
- Model with measurement operator

$$\boxed{\Phi = \mathbf{G}\,\mathbf{F}\,\mathbf{D}\,\mathbf{Z}} \, ,$$

where we incorporate:

- convolutional gridding operator $\mathbf{G}$;
- fast Fourier transform $\mathbf{F}$;
- normalisation operator $\mathbf{D}$ to undo the convolution gridding;
- zero-padding operator $\mathbf{Z}$ to upsample the discrete visibility space.

Supporting continuous visibilities

Algorithm

- Ideally we would like to model the continuous Fourier transform operator

$$\Phi = \mathbf{F}^{\mathrm{c}} .$$

- But this is impractically slow!
- Incorporated gridding into our CS interferometric imaging framework (Carrillo *et al.* 2014).
- Model with measurement operator

$$\Phi = \mathbf{G}\,\mathbf{F}\,\mathbf{D}\,\mathbf{Z} ,$$

where we incorporate:

  - convolutional gridding operator $\mathbf{G}$;
  - fast Fourier transform $\mathbf{F}$;
  - normalisation operator $\mathbf{D}$ to undo the convolution gridding;
  - zero-padding operator $\mathbf{Z}$ to upsample the discrete visibility space.

Supporting continuous visibilities

Algorithm

- Ideally we would like to model the continuous Fourier transform operator

$$\boxed{\Phi = \mathbf{F}^{\mathrm{c}}} \; .$$

- But this is impractically slow!
- Incorporated gridding into our CS interferometric imaging framework (Carrillo *et al.* 2014).
- Model with measurement operator

$$\boxed{\Phi = \mathbf{G}\,\mathbf{F}\,\mathbf{D}\,\mathbf{Z}} \; ,$$

where we incorporate:

  - convolutional gridding operator $\mathbf{G}$;
  - fast Fourier transform $\mathbf{F}$;
  - normalisation operator $\mathbf{D}$ to undo the convolution gridding;
  - zero-padding operator $\mathbf{Z}$ to upsample the discrete visibility space.

Supporting continuous visibilities

Results on simulations

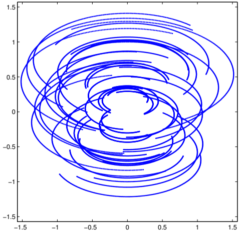

(a) Coverage

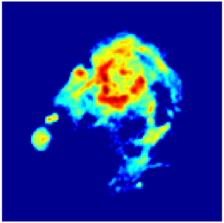

(b) M31 (ground truth)

Figure: Reconstructed images from continuous visibilities.

Supporting continuous visibilities

Results on simulations

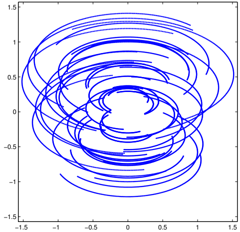

(a) Coverage

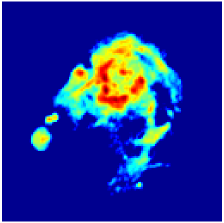

(b) M31 (ground truth)

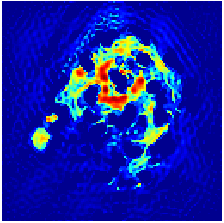

(c) “CLEAN” (SNR= 8.2dB)

Figure: Reconstructed images from continuous visibilities.

Supporting continuous visibilities

Results on simulations

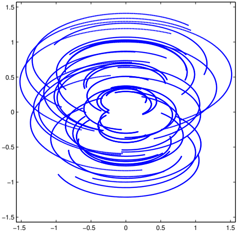

(a) Coverage

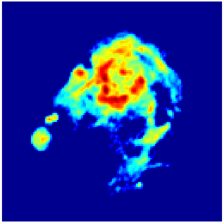

(b) M31 (ground truth)

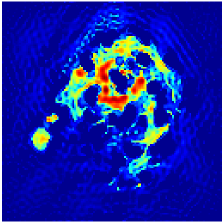

(c) “CLEAN” (SNR= 8.2dB)

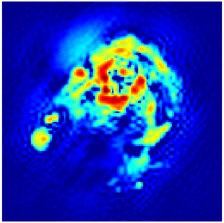

(d) “MS-CLEAN” (SNR= 11.1dB)

Figure: Reconstructed images from continuous visibilities.

Supporting continuous visibilities

Results on simulations

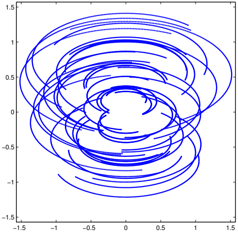

(a) Coverage

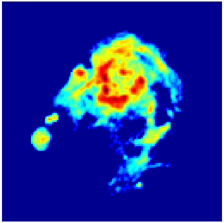

(b) M31 (ground truth)

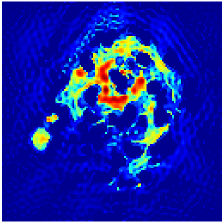

(c) "CLEAN" (SNR= 8.2dB)

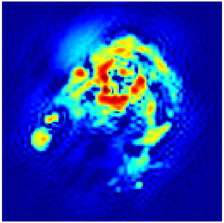

(d) "MS-CLEAN" (SNR= 11.1dB)

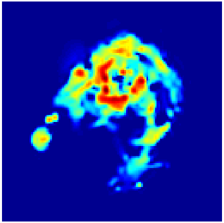

(e) SARA (SNR= 13.4dB)

Figure: Reconstructed images from continuous visibilities.

Spread spectrum effect

Optimising telescope configurations

- Use theory of compressive sensing to optimise telescope configurations.
- Non-coplanar baselines and wide fields $\rightarrow$ w-modulation $\rightarrow$ spread spectrum effect $\rightarrow$ improves reconstruction quality (first considered by Wiaux *et al.* 2009b).
- The w-modulation operator $\mathbf{C}$ has elements defined by

$$C(l,m) \equiv e^{i2\pi w\left(1-\sqrt{1-l^2-m^2}\right)} \simeq e^{i\pi w \|\boldsymbol{l}\|^2} \quad \text{for} \quad \|\boldsymbol{l}\|^4\, w \ll 1 ,$$

giving rise to to a linear chirp.

Spread spectrum effect

Optimising telescope configurations

- Use theory of compressive sensing to optimise telescope configurations.
- Non-coplanar baselines and wide fields $\rightarrow$ w-modulation $\rightarrow$ spread spectrum effect $\rightarrow$ improves reconstruction quality (first considered by Wiaux *et al.* 2009b).
- The w-modulation operator $\mathbf{C}$ has elements defined by

$$C(l,m) \equiv e^{i2\pi w\left(1-\sqrt{1-l^2-m^2}\right)} \simeq e^{i\pi w \|\boldsymbol{l}\|^2} \quad \text{for} \quad \|\boldsymbol{l}\|^4\, w \ll 1 \,,$$

giving rise to to a linear chirp.

Spread spectrum effect

Optimising telescope configurations

- Use theory of compressive sensing to optimise telescope configurations.
- Non-coplanar baselines and wide fields $\rightarrow$ w-modulation $\rightarrow$ spread spectrum effect $\rightarrow$ improves reconstruction quality (first considered by Wiaux *et al.* 2009b).
- The w-modulation operator $\mathbf{C}$ has elements defined by

$$C(l,m) \equiv \mathrm{e}^{\mathrm{i}2\pi w\left(1-\sqrt{1-l^2-m^2}\right)} \simeq \mathrm{e}^{\mathrm{i}\pi w\|\boldsymbol{l}\|^2} \quad \text{for} \quad \|\boldsymbol{l}\|^4\, w \ll 1 \,,$$

giving rise to to a linear chirp.

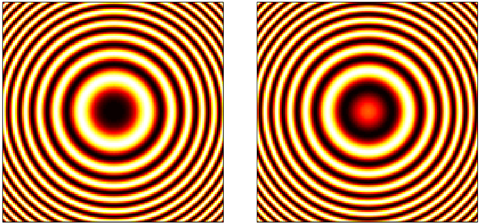

(a) Real part (b) Imaginary part

Figure: Chirp modulation.

Spread spectrum effect

Results on simulations

- Perform simulations to assess the effectiveness of the spread spectrum effect in the presence of varying w.
- Consider idealised simulations with uniformly random visibility sampling.

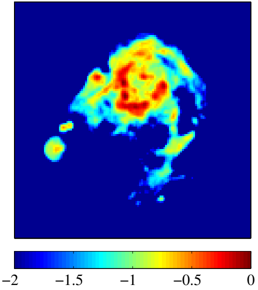

(a) M31

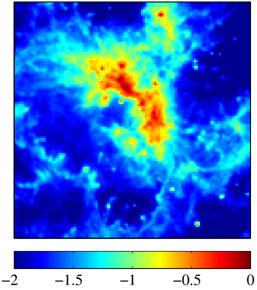

(b) 30Dor

Figure: Ground truth images in logarithmic scale.

Spread spectrum effect

Results on simulations

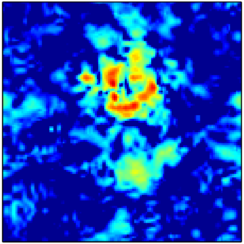

(a) $w_{\mathrm{d}} = 0 \rightarrow$ SNR$= 5$dB

Figure: Reconstructed images of M31 for 10% coverage.

Spread spectrum effect

Results on simulations

(a) $w_d = 0 \rightarrow$ SNR$=$ 5dB

(c) $w_d = 1 \rightarrow$ SNR$=$ 19dB

Figure: Reconstructed images of M31 for 10% coverage.

Spread spectrum effect

Results on simulations

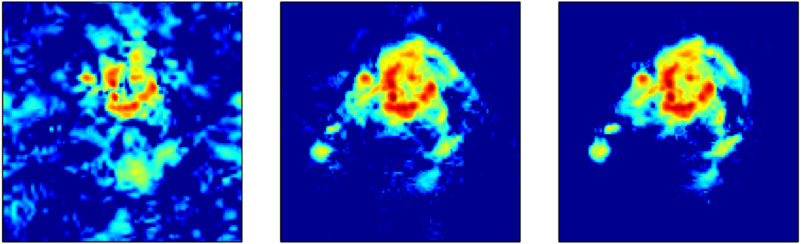

(a) $w_\mathrm{d} = 0 \rightarrow$ SNR$=$ 5dB

(b) $w_\mathrm{d} \sim \mathcal{U}(0, 1) \rightarrow$ SNR$=$ 16dB

(c) $w_\mathrm{d} = 1 \rightarrow$ SNR$=$ 19dB

Figure: Reconstructed images of M31 for 10% coverage.

Spread spectrum effect

Results on simulations

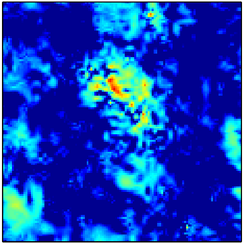

(a) $w_{\rm d} = 0 \rightarrow$ SNR$= 2$dB

Figure: Reconstructed images of 30Dor for 10% coverage.

Spread spectrum effect

Results on simulations

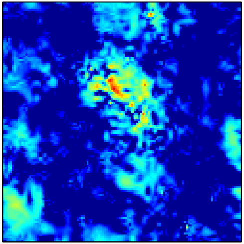

(a) $w_{\mathrm{d}} = 0 \rightarrow$ SNR$=$ 2dB

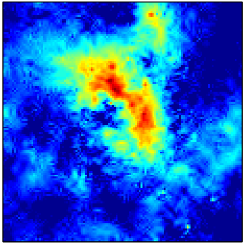

(c) $w_{\mathrm{d}} = 1 \rightarrow$ SNR$=$ 15dB

Figure: Reconstructed images of 30Dor for 10% coverage.

Spread spectrum effect

Results on simulations

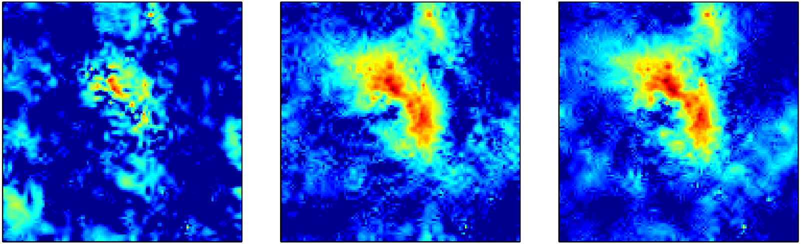

(a) $w_{\mathrm{d}} = 0 \rightarrow$ SNR$= 2$dB (b) $w_{\mathrm{d}} \sim \mathcal{U}(0,1) \rightarrow$ SNR$= 12$dB (c) $w_{\mathrm{d}} = 1 \rightarrow$ SNR$= 15$dB

Figure: Reconstructed images of 30Dor for 10% coverage.

Spread spectrum effect

Results on simulations

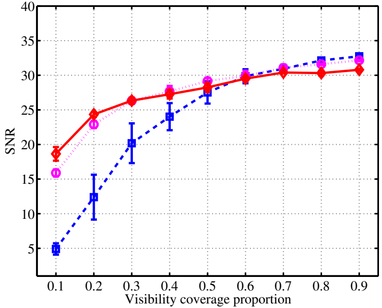

(a) Daubechies 8 (Db8) wavelets

Figure: Reconstruction fidelity for M31.

Improvement in reconstruction fidelity due to the spread spectrum effect for varying w is almost as large as the case of constant maximum w.

- As expected, for the case where coherence is already optimal, there is little improvement.

Spread spectrum effect

Results on simulations

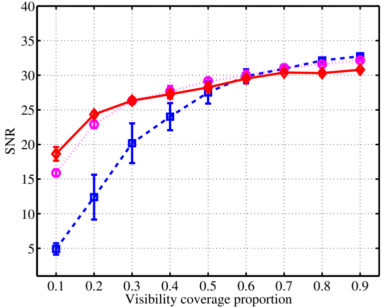

(a) Daubechies 8 (Db8) wavelets

Figure: Reconstruction fidelity for M31.

Improvement in reconstruction fidelity due to the spread spectrum effect for varying w is almost as large as the case of constant maximum w.

- As expected, for the case where coherence is already optimal, there is little improvement.

Spread spectrum effect

Results on simulations

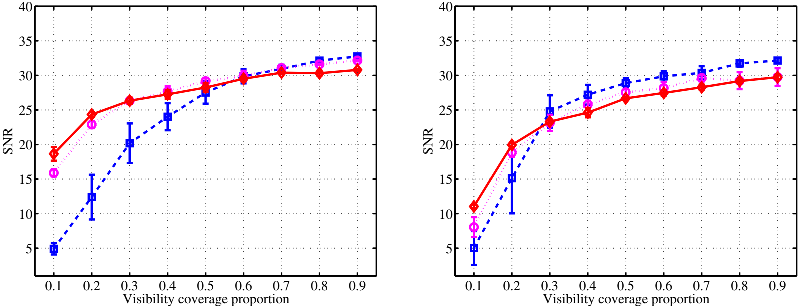

(a) Daubechies 8 (Db8) wavelets (b) Dirac basis

Figure: Reconstruction fidelity for M31.

> Improvement in reconstruction fidelity due to the spread spectrum effect for varying w is almost as large as the case of constant maximum w.

- As expected, for the case where coherence is already optimal, there is little improvement.

Spread spectrum effect

Results on simulations

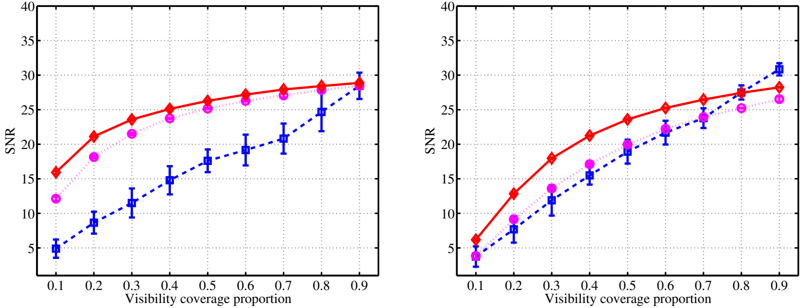

(a) Daubechies 8 (Db8) wavelets (b) Dirac basis

Figure: Reconstruction fidelity for 30Dor.

> Improvement in reconstruction fidelity due to the spread spectrum effect for varying w is almost as large as the case of constant maximum w.

- As expected, for the case where coherence is already optimal, there is little improvement.

Public codes

SOPT code http://basp-group.github.io/sopt/

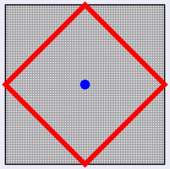

Sparse OPTimisation
Carrillo, McEwen, Wiaux

SOPT is an open-source code that provides functionality to perform sparse optimisation using state-of-the-art convex optimisation algorithms.

PURIFY code http://basp-group.github.io/purify/

Next-generation radio interferometric imaging
Carrillo, McEwen, Wiaux

PURIFY is an open-source code that provides functionality to perform radio interferometric imaging, leveraging recent developments in the field of compressive sensing and convex optimisation.

Conclusions

Astrostatistics is a maturing field.

Informatics techniques (sparsity, wavelets, compressive sensing) are a complementary approach...

...leading to the emerging field of astroinformatics.

Promising approach to radio interferometric imaging for emerging and future radio telescopes.

Extra Slides

Spread spectrum effect
Overview

Spread spectrum effect in a nutshell

1. Radio interferometers take (essentially) Fourier measurements.
2. Recall, the coherence is the maximum inner product between measurement vectors and sparsifying atoms.
3. Thus, coherence is (essentially) the maximum of the Fourier coefficients of the atoms of the sparsifying dictionary.
4. w-modulation spreads the spectrum of the atoms of the sparsifying dictionary, reducing the maximum Fourier coefficient.
5. Spreading the spectrum reduces coherence, thus improving reconstruction fidelity.

- Consistent with findings of Carozzi et al. (2013) from information theoretic approach.
- Studied for constant w (for simplicity) by Wiaux *et al.* (2009b).
- Studied for varying w (with realistic images and various sparse representations) by Wolz *et al.* (2013).

Spread spectrum effect

Sparse w-projection algorithm

- Apply the w-projection algorithm (Cornwell *et al.* 2008) to shift the w-modulation through the Fourier transform:

$$\boxed{\Phi = \mathbf{M}\,\mathbf{F}\,\mathbf{C}\,\mathbf{A} \quad \Rightarrow \quad \Phi = \hat{\mathbf{C}}\,\mathbf{F}\,\mathbf{A}} \; .$$

- Naively, expressing the application of the w-modulation in this manner is computationally less efficient that the original formulation but it has two important advantages.
- Different w for each (u, v), while still exploiting FFT.
- Many of the elements of $\hat{\mathbf{C}}$ will be close to zero.
- Support of w-modulation in Fourier space determined dynamically.

Spread spectrum effect

Results on simulations

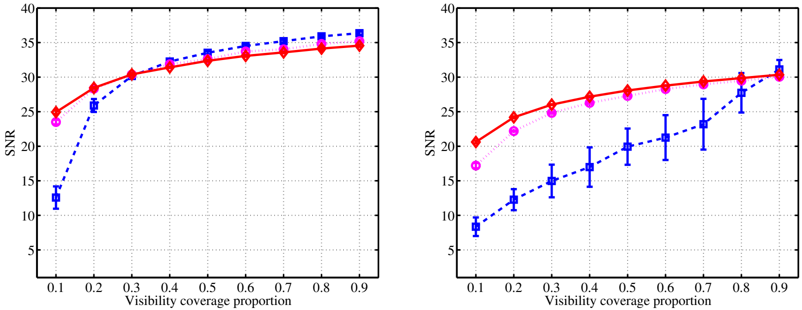

(a) M31 (b) 30 Dor

Figure: Reconstruction fidelity using SARA.

Improvement in reconstruction fidelity due to the spread spectrum effect for varying w is almost as large as the case of constant maximum w.

- As expected, for the case where coherence is already optimal, there is little improvement.